Author Manuscript

Author Manuscript

Author Manuscript

Author Manuscript

HHS Public Access

Author manuscript

J Immunol. Author manuscript; available in PMC 2022 July 15.

Published in final edited form as:

J Immunol. 2021 July 15; 207(2): 505–511. doi:10.4049/jimmunol.2100253.

Anatomic distribution of intravenous injected IgG takes approximately 1 week to achieve stratum corneum saturation in vaginal tissues.

Ann M. Carias[*,#], **Jeffrey R. Schneider**[†,#], **Patrick Madden**[*], **Ramon Lorenzo-Redondo**[‡], **Mariluz Araínga**[§], **Amarendra Pegu**[¶], **Gianguido C. Cianci**[*], **Danijela Maric**[*], **Francois Villinger**[§], **John R. Mascola**[¶], **Ronald S. Veazey**[‖], **Thomas J. Hope**[*]

[*]Department of Cell and Developmental Biology, Feinberg School of Medicine, Northwestern University, Chicago, IL, USA.

[†]Department of Microbial Pathogens and Immunity, Rush University Medical Center, Chicago, IL, USA.

[‡]Department of Medicine, Division of Infectious Diseases, Northwestern University Feinberg School of Medicine, Chicago, IL, 60611, USA.

[§]New Iberia Research Center, University of Louisiana at Lafayette, Lafayette, LA, USA.

[¶]Vaccine Research Center, NIAID, NIH, Bethesda, MD, USA.

[‖]National Primate Research Center, Tulane University School of Medicine, Covington, LA, USA.

Abstract

IV-injected antibodies have demonstrated protection against SHIV infection in rhesus macaques paving the way for the AMP trial where at-risk individuals for HIV received an IV-infusion of the HIV bNAb, VRC01. However, the time needed for these antibodies to fully distribute and elicit protection at mucosal sites is still unknown. Here, we interrogate how long it takes for antibodies to achieve peak anatomical levels at the vaginal surface following IV-injection. Fluorescently-labeled VRC01 and/or Gamunex-C were IV-injected into 24 female rhesus macaques (*Macaca mulatta*) with vaginal tissues and plasma acquired up to 2-weeks post-injection. We found that antibody delivery to the vaginal mucosa occurs in two phases. The first phase involves delivery to the submucosa, occurring within 24hrs and persisting beyond 1 week. The second phase is the delivery through the stratified squamous epithelium, needing approximately 1 week to saturate the

Correspondence may be addressed to: Thomas J Hope, Ph.D. Mailing address: Simpson Querrey Institute 6th floor. 303 E Superior, Chicago, IL 60611. Tel (312) 503-1360. thope@northwestern.edu.

[#]These authors contributed equally

Author contributions:

AMC performed animal experiments, all deconvolution fluorescent microscopy experiments, all image analyses, and co-wrote the manuscript. JRS fluorescently tagged all of the antibodies, conducted all lightsheet microscopy, ran and analyzed all plasma data, and co-wrote the manuscript. PM ran the neutralization assay for VRC01. GCC created the IDL code for MFI analyses. JRM and AP created all VRC01 antibodies used. RLR analyzed biostatistical data. DM developed the tissue clearing methodology for lightsheet microscopy. FJV supervised the animal studies and MA performed animal experiments at NIRC. RSV supervised the animal studies at TNPRC. TJH conceived and supervised all studies and edited the manuscript. All authors discussed and approved the manuscript.

Competing Interests: There are no competing interests to disclose.

Author Manuscript Author Manuscript Author Manuscript Author Manuscript

stratum corneum. This study has important implications for the efficacy of immunoprophylaxis targeting pathogens at the mucosa.

Introduction:

There are currently ~38 million people living with HIV today and ~2 million new HIV infections each year (1). The majority of HIV-1 infection occurs through heterosexual sex, with a larger risk of transmission from male to female (2). One of the more recent clinical trials for an HIV vaccine, HVTN702, was halted due to lack of efficacy, highlighting the need for alternative strategies to prevent HIV infection (3). One possible approach is through the use of broadly neutralizing antibodies (bNAbs), and over the past decade, a growing number of potent, anti-HIV bNAbs have been isolated from HIV-1 infected individuals (4). A large number of these antibodies have been illustrated to sufficiently block infection from a high dose SHIV challenge in non-human primates (NHP) and are currently being tested in human clinical trials (5)(reviewed by (6)) However, although these studies have illustrated protection, the mechanism(s) of IV-injected antibody distribution and localization and how long after bNAb IV infusion their presence persists and mediates protection, especially at mucosal sites where HIV transmission occurs, has not been elucidated. Therefore, understanding the basic mechanisms behind antibody distribution and localization in tissues is extremely significant as it will provide an understanding of how to optimize vaccine responses and passively transferred bNAbs for greater and longer protection against pathogens, including HIV.

Antibody kinetics *in vivo* have been clearly shown to peak in the plasma around 4–6 hours post IV injection and fall precipitately thereafter (7); however, the tissue kinetics of antibody distribution following IV injection are not well defined. Only by elucidating the distribution and localization events of antibodies in tissues, especially those mucosal tissues susceptible to HIV ingress, can strides be made to further develop a therapeutic monoclonal antibody regimen to prevent HIV acquisition and transmission. Therefore, to better understand the localization and distribution of IV-injected antibodies, we developed a platform for tracking passively infused, fluorescently tagged antibodies in rhesus macaques. Using the polyclonal antibody, Gamunex-C, we found that a minimal degree of labeling (~1 fluor/Ab) did not alter antibody biodistribution or function while illustrating our capability of labeling large amounts of antibodies to facilitate macaque studies (8). After injection, we collected mucosal swabs, and vaginal and rectal biopsies and were able to follow the distribution of antibodies over time, providing a unique perspective to observe how Gamunex-C reached different anatomical sites. These exploratory studies have provided novel insights into mechanisms of antibody delivery to different organs and tissues after IV injection into multiple animals.

However, in our previous study, we only looked at Gamunex-C, which is nothing more than pooled polyclonal human IgG. Ultimately, we are interested in identifying how HIV-specific monoclonal antibodies distribute and localize *in vivo* and whether these antibodies are able to reach those mucosal sites most susceptible to HIV ingress, such as the vaginal epithelium of the female reproductive tract (FRT). Therefore, we used our antibody-tracking

Author Manuscript Author Manuscript Author Manuscript Author Manuscript

platform to track VRC01 IgG1 (VRC01). VRC01 is a bNAb directed to the HIV envelope CD4-binding site and has been shown to prevent lentiviral infection in the NHP model (9). This particular bNAb is also being utilized in the ongoing first clinical trial for “Antibody Mediated Prevention” (AMP) aimed at preventing HIV acquisition (10).

With this novel platform, we are able to follow antibody distribution and localization in the NHP model in conjunction with imaging methods, such as fluorescent deconvolution microscopy and lightsheet microscopy. These techniques, combined, have allowed us to evaluate the tissue distribution of IV injected antibodies at both the tissue and cellular level. Here, we present data utilizing fluorophore-labeled Gamunex and VRC01 IgG1 in the living NHP model that provides mechanistic insight into how antibodies distribute and localize to various tissues with an emphasis on vaginal tissues.

Materials and Methods:

Antibody Generation and Fluorescent Labeling:

VRC01 antibodies were donated by John Mascola at the Vaccine Research Center. Gamunex-C (Grifols) was purchased from the Northwestern University Pharmacy. VRC01 and Gamunex-C antibodies were fluorescently labeled by previously established methods (8). In brief antibodies were diluted in PBS down to 25mg/ml in 5mls and buffer exchanged into PBS using a 10ml 40kDa cutoff Zeba column (Thermo-Fischer). Following buffer exchange, Sodium Bicarbonate was added for a final concentration of 100mM and then 2mgs of Cy5 or Cy3 NHS Ester were added (sulfocyanine 5 or sulfocyanine 3 NHS ester, Lumiprobe). This reaction was gently rocked in the dark for 1hr. Following this reaction, the labeled antibody was put through two 10-mL 40kDa Zebra columns, buffer exchanged with PBS, to remove free dye. Labeled antibodies were then passed through a 0.45 filter and stored at 4ºC protected from light. Labeling efficiency was evaluated via SDS PAGE and nanodrop to assess the degree of labeling (fluorophores per antibody) as previously described (8).

Plasma Antibody Measurements:

Fluorescent antibodies in the plasma were measured on the Fluostar Optima (BMG Labtech) using the Cy5 or Cy3 filters. Undiluted plasma samples were added at 100μl per well in duplicate. Using pre-injection Cy5 or Cy3 antibody inoculum, a standard curve was generated and IgG levels were determined using a 4-parameter fit.

Virus Neutralization Assay:

Pseudotyped R9-BaL-mCherry-HIV-1 virus was produced by co-transfection of two plasmids (R9-BaL and mCherry-VPR) into HEK293T cells. Viral supernatants containing pseudotyped virus were collected 48hrs post-transfection, purified through 0.22μm syringe filters, and concentrated over 30% sucrose cushions. TZM-bl cells were used to test neutralization potential of labeled or unlabeled VRC01 against the pseudotyped virus as described previously (11)

Author Manuscript Author Manuscript Author Manuscript Author Manuscript

Ethics Statement:

In total, 24 female macaques (*Macaca mulatta*) were used for this study. All macaques were housed at the Tulane National Primate Research Center (TNPRC) or at the New Iberia Research Center (NIRC) in accordance with the "Guide for the Care and Use of Laboratory Animals". Both the TNPRC and NIRC are fully accredited by the Association for Assessment and Accreditation of Laboratory Animal Care International. All primate studies at TNPRC were reviewed and approved by the Tulane University Institutional Animal Care and Use Committee under protocol numbers P0240R. All primate studies at NIRC were reviewed and approved by the Institutional Animal Care and Use Committee of the University of Louisiana at Lafayette under protocol number 2017–8786-002. At both facilities, rhesus macaques were provided with Monkey chow and water ad libitum supplemented with fruits, vitamins, and Noyes' treats (Research Diets, New Brunswick, NJ). All clinical procedures were carried out under the direction of a laboratory animal veterinarian and were performed under anesthesia using ketamine, often in combination with telazol, with all efforts made to minimize stress, improve housing conditions, and to provide enrichment opportunities (e.g. objects to manipulate in cage, varied food supplements, foraging and task-oriented feeding methods, interaction with caregivers and research staff).

Rhesus macaques:

At TNPRC, 22 animals were administered fluorescently labeled VRC01-WT (VRC01), or a combination of VRC01-WT and VRC01-LS, Human serum albumin (HSA) and Gamunex-C, VRC01-WT and Gamunex-C, or Peptide: N-Glycosidase F (PNG) treated Gamunex-C and Gamunex-C intravenously. Injected antibody concentrations ranged from 12.5mg/kg to 50mg/kg per antibody. A subset of animals had serial vaginal biopsies collected at 24hrs, 48hrs, 72hrs, 1-week and/or up to 2-weeks post antibody administration. Fourteen of the 22 animals were necropsied by 1-week post antibody injection. At NIRC, 2 animals were injected intravenously with 20mg/kg VRC01-WT-Cy3 and VRC01-LS-Cy5 (40mg/total). 72hrs post injection, animals were necropsied and vaginal tissues collected. Specific details on antibody administration for each individual animal can be found in Supplemental Table 1. For vaginal biopsies, tissues were placed into optimal cutting temperature (OCT) and stored at −80°C. Necropsy tissues were processed in one or both of the following ways: 1) tissues were placed in 4% paraformaldehyde (PFA) for future tissue clearing experiments for lightsheet microscopy 2) tissues placed in OCT for fluorescent microscopy. All PFA samples were stored at 4°C; OCT samples were stored at −80°C. When applicable (i.e. based on necropsy time point), plasma was also collected at 0hrs, 24hrs, 48hrs, 72hrs, 1-week and 2-weeks post antibody administration. All samples were shipped overnight to Northwestern University.

Immunofluorescence:

Frozen tissue sections (10–12μm) were fixed in 3.7% formaldehyde in PIPES [piperazine-N,N'-bis(2-ethanesulfonic acid)] buffer for 5 to 10 min followed by washing in cold PBS. Samples were blocked with normal donkey serum for 10 min and washed again. To identify adherens junctions an anti-HECD-1 protein antibody (BD Biosciences), directly conjugated to 488 was applied for 1hr at RT prior to washing. Finally, Hoechst DAPI (4',6-diamidino-2-

Author Manuscript Author Manuscript Author Manuscript Author Manuscript

phenylindole) (Invitrogen) was applied for 10 min to stain nuclei before a final wash with PBS. Mounting medium (DakoCytomation) and coverslips were applied to sections, sealed with clear nail polish, and stored at 4°C until imaged.

Deconvolution Microscopy and Image Analysis:

Images were obtained by deconvolution microscopy on a DeltaVision RT system collected on a digital camera (CoolSNAP HQ; Photometrics) using a 40X or 100X oil objective. To fully visualize antibody localization and distribution in vaginal tissues over time, we took up to 5 images of vaginal tissue from each macaque. Panel images were acquired to include the epithelium and lamina propria. Each image consisted of a stitched panel comprised of three 40X images across the tissue surface and several 40X images past the basal layer, depending on the epithelial thickness of each sample. ImageJ/FIJI software was used to calculate the percentage of stratum corneum with fluorescently tagged antibodies (see Supplemental Figure 1A). For these analyses, first the area of the stratum corneum, as characterized by the absence of adherens junctions, was taken. Next, the total area of fluorescent antibody within the stratum corneum was measured. Afterwards, dividing the area of detectable antibody by the total stratum corneum area and multiplying by 100, calculated the percentage of antibody within the non-viable stratum corneum. For mean fluorescent intensity analyses, single, non-panel z-scan stacks were collected over 15μm for each image field at 100X, and image analysis was performed with using in-house algorithms written in IDL 8.1 (Harris Geospatial Solutions) and the Bio-Formats library (12). For each sample, approximately 10 z-scan stack images were randomly obtained within the lamina propria of the vaginal tissues. The regions imaged were 60μm wide and 12μm thick.

Tissue clearing and lightsheet microscopy:

Following necropsy, tissues were fixed in 4% paraformaldehyde for 24hrs at 4° C. Tissues were cleared following an established protocol (13, 14). Following fixation tissues were rinsed 2 times in PBS followed by dehydration by exchanging the buffer to increasing tert-butanol (#360538, Sigma) concentrations (30%, 50%, 80, 96, 100%). Each buffer exchange of tert-butanol was incubated for 24hrs at 30°C. Following, the last Tert-butanol exchange, Tissues were placed in Hexane for 1hr at 30°C followed by incubation in BABBS solution for 24hrs at 30°C. Tissues were buffer exchanged with 2 more rounds of fresh BABBS buffer solution for 24hrs at 30°C prior to imaging. BABBS solution is 1 part benzyl alcohol (#13160, Sigma) and 2 parts benzyl benzoate (#B6630, Sigma). All alcohol and BABBs solutions were set at pH 9.5 using triethylamine (#471283, Sigma). Tissues were imaged in BABBs solution on a LaVision Ultramicroscope II with zoom configuration. Following acquisition, images were processed using ImageJ and Imaris reconstruction software. In all images, green represents tissue autofluorescence and red represents the fluorophore-conjugated antibody.

Statistical Analyses:

Statistical analyses were performed using R version 4.0.2. To test for differences in the percentage of antibody in the total SC area between the two antibodies tested through time, we used a Zero-One-Inflated Beta model using the gamlss R package. We selected this type of model as the best suited for our antibody covered area percentage data that

Author Manuscript Author Manuscript Author Manuscript Author Manuscript

includes 0 and 1 (0 for 0% area covered by antibody and 1 for 100% percent covered). We estimated the effects of time, antibody, and their interaction in the model and tested for statistically significant differences in all the possible contrasts within the model. We used Benjamini Hochberg method for multiple testing correction and the false discovery rate adjusted p-value (q-value) for statistical significance was set at q-value <0.05.

Results:

There are minimal differences between Gamunex-C and VRC01 distribution and localization in the vaginal epithelium:

As mentioned above, we previously demonstrated that upon administration to animals fluorescently tagged Gamunex-C behaved comparably to unlabeled Gamunex-C as far as antibody distribution within tissues. One of the anatomical tissues we previously assessed was the vaginal epithelium. We found that antibodies, both endogenous and injected Gamunex-C, were present primarily within the lamina propria and stratum corneum, while the viable stratum malpighii did not exhibit a strong IgG fluorescent signal (8). It was unclear whether bNAbs, such as VRC01, also distribute to these epithelial layers similarly. Therefore, we set out to investigate if there were differences in VRC01 antibody localization and distribution within the vaginal epithelium after IV-injection. To gain insights into this process, we fluorescently tagged Gamunex-C with Cy5 and VRC01 with Cy3 dyes. The labeling efficiency is shown for VRC01-Cy3 through resolution on SDS PAGE under reducing conditions (Supplemental Figure 1B). Of note, this labeling did not alter HIV neutralization activity in a TZM-bl assay (Supplemental Figure 1C).

We injected a single rhesus macaque (animal EC74 – see Supplemental Table 1) with both fluorescently-labeled Gamunex-C (Cy3) and VRC01 (Cy5) (12.5mg/kg for each antibody) simultaneously. Vaginal biopsies were then collected at 24, 48, 72hrs, and 1-week post-antibody infusion, embedded in OCT, and imaged with deconvolution fluorescent microscopy. After imaging vaginal biopsy tissues from each time point, we did not see a difference between Gamunex and VRC01 IgG1 distribution and localization. For example, at 24hrs post-infusion, both Gamunex-C and VRC01 were found to overlap in the same image, with both antibodies appearing in the lamina propria and areas of the stratum granulosum (Supplemental Figure 1D). These data suggest that these distribution patterns and events are alike regardless of antibody clonality or type.

It takes approximately 1 week for antibodies to reach steady state saturation in the vaginal epithelium:

After injection, we monitored how antibodies reached the vaginal luminal surface to offer protection. Tracking fluorescently labeled Gamunex-C and VRC01 localization with sequential biopsies from the same animal (EC74) up to a week following passive infusion, we found that both antibodies entered the squamous vaginal epithelium from the lamina propria, through the basal layer, and migrated quickly through the spinosum to the granulosum where the epithelial cells undergo programmed cell death and degrade to form the stratum corneum from the bottom up. The timed injection of the fluorescently labeled antibody functions as a pulse into a continuously ongoing process of building the stratum

Author Manuscript Author Manuscript Author Manuscript Author Manuscript

corneum from the bottom up while also shedding the degraded cell husks from the luminal surface. This process is initiated within 24 hours and reaches a steady state of tissue saturation by one week (Figure 1A–H). As illustrated in Figure 1, the four time points depict the stratified squamous epithelium with the green line denoting the boundary between the spinosum and granulosum, while the white line denotes the lumen. The area between these two lines is the stratum corneum, also known as the non-viable layer. IV-injected antibody fluorescence, as depicted in red, slowly builds up in this layer, completely saturating the stratum corneum by 1-week post-injection (Figure 1D, H).

To gain insight into the variability of the kinetics of antibody entry into the stratum corneum, we acquired vaginal tissues from additional rhesus macaques from other ongoing studies that were IV-injected with 12.5, 25, or 50mg/kg of fluorophore-conjugated VRC01 or Gamunex-C (see Supplemental Table 1). Once again, we imaged vaginal tissues from individual animals, both biopsies and necropsy tissues at 24hrs, 48hrs, 72hrs, and 1-week post-injection through deconvolution microscopy. From each of these images, we were able to quantify the percentage of Gamunex-C and VRC01 within the non-viable stratum corneum to determine the time needed, post IV injection, for antibodies to come to a steady state distribution throughout the stratum corneum of the vaginal epithelium and reach the surface to provide protection against invading pathogens (Figure 1I). For example, at 24hrs post-injection, we found that both Gamunex-C and VRC01 traveled less than 25% through the stratum corneum to reach the luminal surface (14.38±12.33 and 14.60±11.1, respectively). At 48 hours Gamunex-C and VRC01 only made it through ~40% (41.49±17.1 and 42.74±16.99, respectively) of the non-viable stratum corneum. At 72hrs, there was a high level of heterogeneity between animals, regardless of injected antibody with Gamunex-C filling ~94% (94.37±33.08) amount of the stratum corneum and VRC01 covering only ~44% (44.41±26.92). However, at 1 week, both Gamunex-C and VRC01 reached a steady state, both at 100% (100±2.92 and 100±3.34, respectively) (Figure 1I). Of note, any differences between Gamunex-C versus VRC01 are likely due to heterogeneity amongst animals because when Gamunex-C and VRC01 were in the same animal they distributed together as shown in Figure 1 and Supplemental Figure 1. Importantly, there were no statistically significant differences between the percentage amounts of Gamunex-C versus VRC01 that saturated the stratum corneum at each time point; thereby illustrating that this 1-week steady state phenomenon was not affected by antibody clonality and/or type (Figure 1I).

To visualize antibody distribution in larger pieces of tissue to ascertain whether this 1-week steady state was widely true for the vaginal epithelium, we utilized lightsheet microscopy to visualize centimeter pieces of tissue to tease out mechanisms of antibody distribution at the organ level. In doing so, 3 additional rhesus macaques (CJ89, GA04, AF94) were once again IV-injected with 25mg/kg (CJ89 and GA04) or 20mg/kg (AF94) (see Supplemental Table 1) fluorophore-conjugated VRC01 and animals were sacrificed at 24hr, 48hrs, and 72hrs after which tissue was isolated. After isolation, vaginal tissue was clarified prior to imaging using established protocols (13, 14) and imaged on a LaVision lightsheet microscope whereby large z-stacks were acquired and reconstructed to get a 3D view of antibody distribution. Using a z-stack reconstitution of these images, we were able to once again visualize the temporal movement of antibody through the vaginal squamous epithelium, except this time

Author Manuscript Author Manuscript Author Manuscript Author Manuscript

at the whole tissue/organ level. (Video 1, Figure 1J–L). Figure 1J–L, from left to right illustrates 24, 48, and 72hrs post IV injection. In each successive image, the antibody band moved further into the epithelium, closer to the vaginal epithelial surface, as depicted by the white arrows. Unfortunately, due to budgetary restrictions, we only had resources for three macaques for this study, but it is evident that IV-injected antibodies are slowly building in the vaginal epithelium from the lamina propria to the luminal vault, which correlates with our deconvolution microscopy data.

Temporal distribution of antibodies is not the same for plasma and vaginal tissue:

One of the questions that remained was whether antibody levels in the plasma correlated with IV-injected fluorescently-labeled antibodies found within the vagina. To address this question, we collected plasma and vaginal tissue samples from ten rhesus macaques (JA24, IN98, HD66, EN39, IG91, JB10, FH82, JC11, IN68 and FG38 – see Supplemental Table 1) passively infused with VRC01-Cy3 or VRC01-Cy5. To measure the amount of antibody in the vagina, we utilized custom image analysis algorithms previously developed in our laboratory, that allow us to quantify the mean fluorescent intensity of fluorescently labeled antibodies in various tissues in a high throughput manner (8). Importantly, since we found that antibodies need ~1 week to saturate the vaginal squamous epithelium, we only measured fluorescent antibodies that were present beneath the vaginal epithelium, within the lamina propria, which showed steady state between 1 and 7 days (Figure 2A). Next, we measured the plasma levels of IV-injected antibodies from the same animal set. A standard curve was derived for Cy3 and Cy5 labeled VRC01, to quantify antibody levels in the plasma. Plasma levels of labeled VRC01 showed a steady decline from 24hrs, 48hrs, 72hrs, 1-week and 2-weeks, post-injection (Figure 2B). The ratio of fluorescently-tagged antibody plasma concentration versus vaginal tissue mean fluorescent intensity, therefore dropped between 24hrs and 1 week (Figure 2C), which combined with Figure 1I, suggest that during the timeframe of 24hrs to 1 week, antibody is promptly leaving the circulation, entering the submucosal tissue, where it slowly enters the tissue epithelium to reach saturation in the vaginal tissue around 1-week post IV injection.

Discussion:

Therapeutic monoclonal antibodies (mAbs) have permeated every disease setting in the clinic due to their safety and efficacy. While traditional production of mAbs remains expensive, the ability to clone and express human mAbs in plant and yeast based production systems are paving the way towards large-scale cost effective production with defined quality control (15, 16). These developments make it possible to use mAb based prevention protocols for a number of infectious disease such as HIV, as currently trialed with bNAb, VRC01 (AMP study). However, while the therapeutic administration of mAbs will ultimately select existing targets, establishing a anti-infective barrier at mucosal portals of entry requires localization and distribution to such anatomical sites, a property that has until yet not been addressed in much detail. Hence, the rationale for the study described here utilizes two novel techniques recently developed in our laboratory. The first is the use of a directly labeled antibody platform, thereby allowing for direct observation of antibody distribution after infusion in an *in vivo* system. Additionally, directly labeling these

Author Manuscript Author Manuscript Author Manuscript Author Manuscript

antibodies permit for a highly sensitive assessment of antibody levels throughout vaginal epithelial tissues. The second innovation is the use of various microscopy techniques, such as deconvolution fluorescent and lightsheet microscopy, to observe antibody distribution and localization at both the micron and centimeter scales in samples of tissue.

After injection of both polyclonal Gamunex-C and bNAb VRC01, each tagged with a different color fluorophore, we see that the mechanism(s) of antibody distribution and localization in the vaginal epithelium is the same regardless of any Fc differences, clonality and/or antibody type (Supplemental Figure 1C). Additionally, here we illustrate that we are successful in following antibody distribution over time, to provide a unique perspective in observing where antibodies accumulate and how antibodies reach different anatomical sites. For example, through tracking fluor-labeled antibody distribution with sequential biopsies, we illustrate that antibody initially enters the squamous vaginal epithelium from the lamina propria, through the basal layer, moving quickly through the spinosum, undergoing programmed cell death at the granulosum and accumulating in the stratum corneum from the bottom up (Figure 1). Through this bottom loading process, we can measure a steady-state distribution throughout the stratum corneum that is achieved at ~1-week post-administration with close to 100% antibody saturation (Figure 1I). Also of note, in this study, we illustrate that antibody levels decrease in the plasma and concurrently accumulate and persist in the vaginal tissue over time, which illustrates that antibody kinetics in plasma are not identical to tissue and should be treated as separate entities (Figure 2). Importantly, we found a novel mechanism of antibody delivery to the squamous vaginal mucosa as both data combined (Figure 1, 2), suggests that antibody distribution into the vaginal mucosa occurs in two phases after IV-injection.

During the first phase, we find that by 24hrs, antibody from the plasma leaves the vascular system and fills the vaginal lamina propria. These data correspond with previously published data that illustrates antibodies leaving the plasma and entering the interstitium through a process called convective extravasation (17, 18). Convective extravasation occurs due to differences in pressure gradients of the vascular and tissue environments and is considered to be the primary mechanism of bNAb delivery into tissues (17). Although another possible mechanism of antibody delivery to the vaginal lamina propria could be due to FcRn-mediated transcytosis, it is unlikely that this tissue delivery mechanism plays a large role in our observations as it has been reported that IgG distribution and tissue delivery is still evident in FcRn- knockout mice after IV administration of 7E3 (19). However, to examine the role FcRn-mediated transcytosis may have on antibody delivery to the vaginal lamina propria, we are currently in the process of analyzing tissues from animals co-injected with VRC01 and VRC01-LS, with the latter being modified form of VRC01 that has increased affinity to FcRn thereby resulting in a longer antibody half-life (9).

During the second phase, following convective extravasation into the lamina propria, we illustrate here that antibody is picked up by basal epithelial cells and travels to the luminal cavity through squamous cell differentiation, which takes ~1 week. By 1 week, we find a clear stabilization of antibody distribution where antibody is minimal in plasma, but highly evident in the lamina propria and epithelium of vaginal squamous tissues (Figure 2C). Previously, through IHC techniques, this squamous epithelia antibody distribution

Author Manuscript Author Manuscript Author Manuscript Author Manuscript

phenotype was reported in the epithelia of tonsils and anal tissues (20). Likewise, we have noted similar results in other mucosal squamous epithelia, such as the oral buccal and inner foreskin tissues (data not shown), thereby suggesting that this mechanism is not just vaginal specific but occurs in most, if not all, squamous tissues. Above all, our results provide ample evidence that currently established antibody distribution models, such as the minimally physiologically-based pharmacokinetic model (mPBPK), may not be ideal for defining the pharmacokinetics for squamous tissues as although these areas may be defined as tissues with tight junctions as a whole (lamina propria and epithelium), antibody distribution between the lamina propria and epithelium are drastically different (21, 22).

The two-phase antibody distribution to the vaginal epithelium described in this study also helps clarify previous results looking at the time course of antibody levels in vaginal secretions following IV injection. Specifically, in previous work by Klein et al., antibody levels spiked in vaginal secretions around 4–6 hours after IV injection, followed by a sudden decrease, and then another spike around 48–72hrs post-injection (7). In our previous study, we also observed similar results whereby we saw an initial spike of fluorescently-labeled antibodies ~2–4hrs after IV injection, followed by a sudden decrease, with a second antibody influx around 1-week post-IV injection (8). One potential explanation for this phenomenon is that the first increase in antibodies found in vaginal fluids could be antibody coming from the upper FRT – an anatomical area that is mostly comprised of simple columnar epithelia. Seeing how we can visualize antibody within the submucosa as soon as 24hrs post-antibody injection, we hypothesize that these antibodies can cross the single-celled barrier of the simple columnar epithelia to empty into FRT luminal spaces at early time points. Next, we believe the second antibody spike found in vaginal fluids originates from tissues of the lower FRT, via the two-phase antibody distribution mechanism discussed in this study. Regardless, to understand this further, we are currently examining antibody distribution dynamics in simple columnar tissues, such as the endocervical and uterine mucosa of the upper FRT. Moreover, in conjunction with these ongoing studies, we are also including other tissues of interest in our analyses, such as lymph nodes and gastrointestinal tissues.

Overall, our data highlight an important point for challenge studies that only give 24hrs of antibody treatment before vaginal challenge, being that this site of challenge may not be optimally protected. This was realized in the Liu et al., study, whereby rhesus macaques were given PGT121 24hrs before intravaginal challenge with SHIV-SF162P3 and the site of challenge had viral RNA and DNA detected 1–3 days post-challenge, which decreased by 7 days, and eventually cleared 10 days later (23). Therefore, we speculate that by giving a week for antibodies to accumulate at the site of challenge it is possible to enhance protection. We would hypothesize a marked decrease in viral RNA and DNA in the vaginal tissue during these early time points after challenge (1–3 days). These data presented here also corroborate important findings from the Haigwood lab, which also showed that it takes time for antibody to clear the infection (24). In these experiments, antibody was IV administered shortly after oral SHIV exposure, but virus was still detected in tissues 2 days post-infection. The 2-week time point cleared the virus, when the next serial necropsy was taken, highlighting the idea that antibody needs more time (e.g. 1 week) to get through and saturate the squamous epithelia to interact with the virus. Alternatively, in studies where

Author Manuscript Author Manuscript Author Manuscript Author Manuscript

virus is challenged intravenously 1hr post-antibody administration, such as in Parsons et al., it is logical that this short duration of time would be adequate to block systemic infection, as IV-injected antibodies would be able to interact with and neutralize the virus, in the blood, prior to virus reaching the tissue (25). These studies, together, stress the critical role of the timing of antibody distribution.

Importantly, our study highlights the critical role of the timing of antibody distribution with our results having major clinical implications for current and future ongoing human antibody infusion trials by illustrating that a week may be required for optimal protection to occur at specific mucosal surfaces from invading pathogens. Additionally, by waiting at least a week to allow for antibody distribution is more similar to vaccine-induced antibodies, which would be secreted continuously and in a steady state distribution. It is only through elucidating the mechanism(s) of the distribution and localization of fluorescently tagged antibodies that future vaccine efforts could be better targeted to provide protection at relevant HIV mucosal sites, such as the vaginal vault. Such understanding will also facilitate optimization of the use of passively transferred antibodies aimed to protect against HIV more efficiently. Here, we provide a novel perspective because although numerous studies are being performed to look at how bNAbs offer sterilizing protection to various pathogens, including HIV/SHIV, this is the first study that examines the potential mechanisms behind such protection.

Supplementary Material

Refer to Web version on PubMed Central for supplementary material.

Acknowledgments:

We would like to acknowledge Constadina Arvanitis and David Kirchenbüchler for their assistance with lightsheet microscopy. This work was performed at the Northwestern University Center for Advanced Microscopy generously supported by NCI CCSG P30 CA060553 awarded to the Robert H Lurie Comprehensive Cancer Center. We would also like to acknowledge Patrick Kiser for his assistance and expertise with fluorescent-labeling methodologies.

This work was supported by NIH 1 K01 OD026571-01 (AMC), K01OD024882-01 (JRS), HIVRAD P01AI048240 (TJH), and Center for the Structural Biology of Cellular Host Elements in Egress, Trafficking and Assembly of HIV (CHEETAH) 5P50AI150464-7294 (TJH).

Abbreviations used in this article:

AMP	antibody mediated prevention
bNAb	broadly neutralizing antibody
FRT	female reproductive tract
HIV	human immunodeficiency virus
HSA	human serum albumin
mAb	monoclonal antibody
mPBPK	minimally physiologically-based pharmacokinetic model

Author Manuscript Author Manuscript Author Manuscript Author Manuscript

NHP	non-human primate
NIRC	New Iberia Research Center
OCT	optimal cutting temperature
PFA	paraformaldehyde
PIPES	piperazine-N,N'-bis(2-ethanesulfonic acid)
PNG	Peptide N-Glycosidase F
SHIV	simian human immunodeficiency virus
TNPRC	Tulane National Primate Research Center; VRC01, VRC01 IgG

References

1. UNAIDS. 2020. 2020 Report on the global AIDS epidemic.
2. Shattock RJ, and Moore JP. 2003. Inhibiting sexual transmission of HIV-1 infection. Nat Rev Microbiol 1: 25–34. [PubMed: 15040177]
3. Dieffenbach CW, and Fauci AS. 2020. The search for an HIV vaccine, the journey continues. J Int AIDS Soc 23: e25506. [PubMed: 32418357]
4. Burton DR, and Mascola JR. 2015. Antibody responses to envelope glycoproteins in HIV-1 infection. Nat Immunol 16: 571–576. [PubMed: 25988889]
5. Moldt B, Rakasz EG, Schultz N, Chan-Hui PY, Swiderek K, Weisgrau KL, Piaskowski SM, Bergman Z, Watkins DI, Poignard P, and Burton DR. 2012. Highly potent HIV-specific antibody neutralization in vitro translates into effective protection against mucosal SHIV challenge in vivo. Proceedings of the National Academy of Sciences of the United States of America 109: 18921–18925. [PubMed: 23100539]
6. Julg B, and Barouch DH. 2019. Neutralizing antibodies for HIV-1 prevention. Curr Opin HIV AIDS 14: 318–324. [PubMed: 31082819]
7. Klein K, Veazey RS, Warrier R, Hraber P, Doyle-Meyers LA, Buffa V, Liao HX, Haynes BF, Shaw GM, and Shattock RJ. 2013. Neutralizing IgG at the portal of infection mediates protection against vaginal simian/human immunodeficiency virus challenge. Journal of virology 87: 11604–11616. [PubMed: 23966410]
8. Schneider JR, Carias AM, Bastian AR, Cianci GC, Kiser PF, Veazey RS, and Hope TJ. 2017. Long-term direct visualization of passively transferred fluorophore-conjugated antibodies. Journal of immunological methods 450: 66–72. [PubMed: 28780040]
9. Ko SY, Pegu A, Rudicell RS, Yang ZY, Joyce MG, Chen X, Wang K, Bao S, Kraemer TD, Rath T, Zeng M, Schmidt SD, Todd JP, Penzak SR, Saunders KO, Nason MC, Haase AT, Rao SS, Blumberg RS, Mascola JR, and Nabel GJ. 2014. Enhanced neonatal Fc receptor function improves protection against primate SHIV infection. Nature 514: 642–645. [PubMed: 25119033]
10. Gilbert PB, Juraska M, deCamp AC, Karuna S, Edupuganti S, Mgodi N, Donnell DJ, Bentley C, Sista N, Andrew P, Isaacs A, Huang Y, Zhang L, Capparelli E, Kochar N, Wang J, Eshleman SH, Mayer KH, Magaret CA, Hural J, Kublin JG, Gray G, Montefiori DC, Gomez MM, Burns DN, McElrath J, Ledgerwood J, Graham BS, Mascola JR, Cohen M, and Corey L. 2017. Basis and Statistical Design of the Passive HIV-1 Antibody Mediated Prevention (AMP) Test-of-Concept Efficacy Trials. Statistical communications in infectious diseases 9.
11. Sarzotti-Kelsoe M, Bailer RT, Turk E, Lin CL, Bilska M, Greene KM, Gao H, Todd CA, Ozaki DA, Seaman MS, Mascola JR, and Montefiori DC. 2014. Optimization and validation of the TZM-bl assay for standardized assessments of neutralizing antibodies against HIV-1. Journal of immunological methods 409: 131–146. [PubMed: 24291345]
12. Linkert M, Rueden CT, Allan C, Burel JM, Moore W, Patterson A, Loranger B, Moore J, Neves C, Macdonald D, Tarkowska A, Sticco C, Hill E, Rossner M, Eliceiri KW, and Swedlow JR.

Author Manuscript Author Manuscript Author Manuscript Author Manuscript

2010. Metadata matters: access to image data in the real world. The Journal of cell biology 189: 777–782. [PubMed: 20513764]

13. Kolesova H, Capek M, Radochova B, Janacek J, and Sedmera D. 2016. Comparison of different tissue clearing methods and 3D imaging techniques for visualization of GFP-expressing mouse embryos and embryonic hearts. Histochemistry and cell biology 146: 141–152. [PubMed: 27145961]
14. Parra SG, Vesuna SS, Murray TA, and Levene MJ. 2012. Multiphoton microscopy of cleared mouse brain expressing YFP. Journal of visualized experiments : JoVE: e3848. [PubMed: 23023035]
15. Cao J, Perez-Pinera P, Lowenhaupt K, Wu MR, Purcell O, de la Fuente-Nunez C, and Lu TK. 2018. Versatile and on-demand biologics co-production in yeast. Nature communications 9: 77.
16. Moussavou G, Ko K, Lee JH, and Choo YK. 2015. Production of monoclonal antibodies in plants for cancer immunotherapy. Biomed Res Int 2015: 306164. [PubMed: 26550566]
17. Baxter LT, Zhu H, Mackensen DG, and Jain RK. 1994. Physiologically based pharmacokinetic model for specific and nonspecific monoclonal antibodies and fragments in normal tissues and human tumor xenografts in nude mice. Cancer Res 54: 1517–1528. [PubMed: 8137258]
18. Ryman JT, and Meibohm B. 2017. Pharmacokinetics of Monoclonal Antibodies. CPT Pharmacometrics Syst Pharmacol 6: 576–588. [PubMed: 28653357]
19. Garg A, and Balthasar JP. 2007. Physiologically-based pharmacokinetic (PBPK) model to predict IgG tissue kinetics in wild-type and FcRn-knockout mice. J Pharmacokinet Pharmacodyn 34: 687–709. [PubMed: 17636457]
20. Coruh G, and Mason DY. 1980. Serum proteins in human squamous epithelium. The British journal of dermatology 102: 497–505. [PubMed: 6992842]
21. Cao Y, Balthasar JP, and Jusko WJ. 2013. Second-generation minimal physiologically-based pharmacokinetic model for monoclonal antibodies. J Pharmacokinet Pharmacodyn 40: 597–607. [PubMed: 23996115]
22. Cao Y, and Jusko WJ. 2014. Survey of monoclonal antibody disposition in man utilizing a minimal physiologically-based pharmacokinetic model. J Pharmacokinet Pharmacodyn 41: 571–580. [PubMed: 25146360]
23. Liu J, Ghneim K, Sok D, Bosche WJ, Li Y, Chipriano E, Berkemeier B, Oswald K, Borducchi E, Cabral C, Peter L, Brinkman A, Shetty M, Jimenez J, Mondesir J, Lee B, Giglio P, Chandrashekar A, Abbink P, Colantonio A, Gittens C, Baker C, Wagner W, Lewis MG, Li W, Sekaly RP, Lifson JD, Burton DR, and Barouch DH. 2016. Antibody-mediated protection against SHIV challenge includes systemic clearance of distal virus. Science 353: 1045–1049. [PubMed: 27540005]
24. Hessell AJ, Jaworski JP, Epson E, Matsuda K, Pandey S, Kahl C, Reed J, Sutton WF, Hammond KB, Cheever TA, Barnette PT, Legasse AW, Planer S, Stanton JJ, Pegu A, Chen X, Wang K, Siess D, Burke D, Park BS, Axthelm MK, Lewis A, Hirsch VM, Graham BS, Mascola JR, Sacha JB, and Haigwood NL. 2016. Early short-term treatment with neutralizing human monoclonal antibodies halts SHIV infection in infant macaques. Nat Med 22: 362–368. [PubMed: 26998834]
25. Parsons MS, Lee WS, Kristensen AB, Amarasena T, Khoury G, Wheatley AK, Reynaldi A, Wines BD, Hogarth PM, Davenport MP, and Kent SJ. 2019. Fc-dependent functions are redundant to efficacy of anti-HIV antibody PGT121 in macaques. J Clin Invest 129: 182–191. [PubMed: 30475230]

Author Manuscript Author Manuscript Author Manuscript Author Manuscript

Key Points:

- It takes ~1-week for IV-injected antibodies to saturate the vaginal epithelium.
- Antibody delivery into the vaginal mucosa occurs in two phases.

Author Manuscript Author Manuscript Author Manuscript Author Manuscript

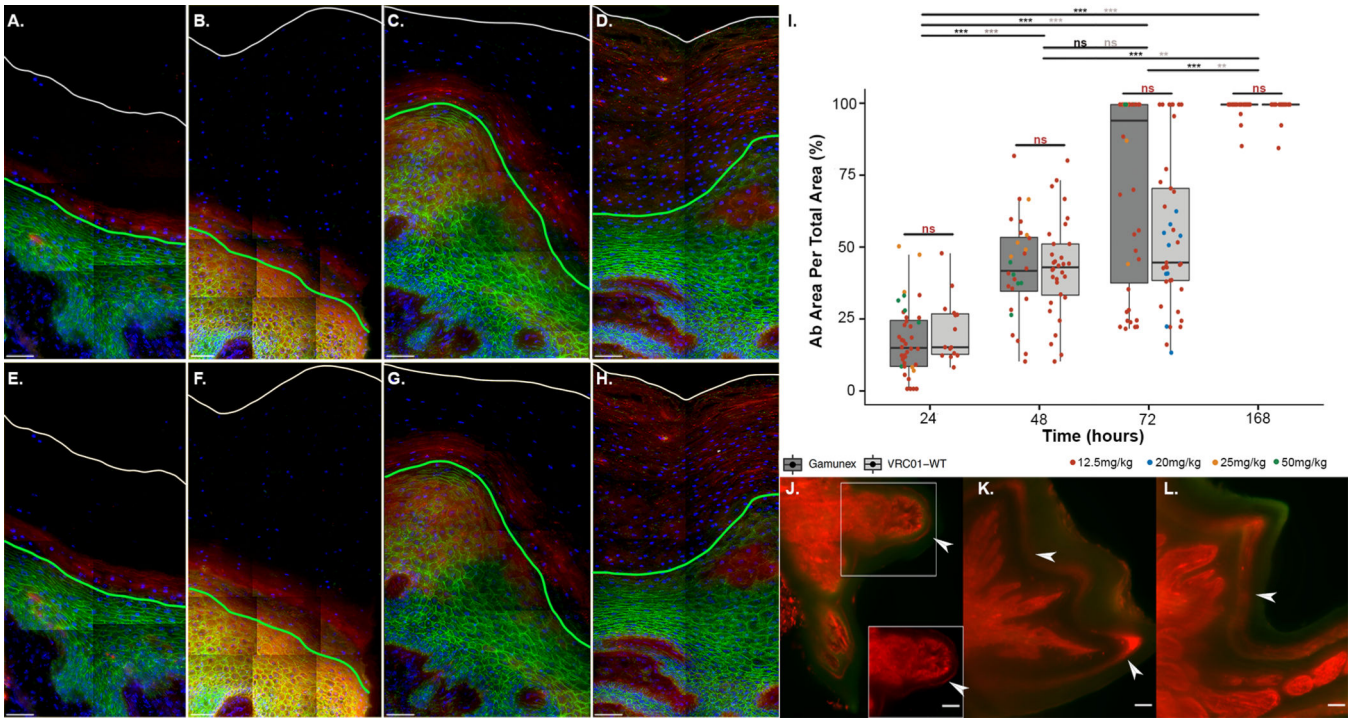

Figure 1: It takes ~1 week for IV-injected antibodies to saturate the vaginal squamous epithelium

(A-H) Fluorescent deconvolution image (40X panels) of vaginal epithelium from animal EC74 after IV-injection of Gamunex-C-Cy3 (top panels) and VRC01-Cy5 (bottom panels) at 24hrs (A, E), 48hrs (B, F), 72hrs (C, G), and 1-week (D, H). Top panels: Gamunex-C-Cy3 (red), E-cadherin (green), and DAPI (blue). Bottom panels: VRC01-Cy5 (red), E-cadherin (green), and DAPI (blue). White lines illustrate the tissue surface. Green lines denote where the viable stratum malpighii begins. The area between the two lines is considered the non-viable stratum corneum. Scale bars are 40μm. (I) Temporal analyses of the percentage of vaginal stratum corneum saturated by IV-injected Gamunex-C (dark gray) or VRC01 (light gray). Each data point represents an image. Data points are colored by antibody injection concentrations of 12.5mg/kg (red), 20mg/kg (blue), 25mg/kg (orange), and 50mg/kg (green). Error bars represent SEM. q-values for Gamunex-C comparisons over time represented in black. q-values for VRC01 comparisons over time represented in gray. q-values for Gamunex-C versus VRC01 at a given time point represented in red. (J-K) Lightsheet microscopy of vaginal epithelium at 24hrs (J), 48hrs (K), and 72hrs (L) post IV injection. Cy3 labeled VRC01 is depicted in red and background fluorescence is depicted in green. Inset image in (J) depicts Cy3-labeled VRC01 without background fluorescence. White arrows indicate the antibody migration front. Scale bar is 100um.

Author Manuscript Author Manuscript Author Manuscript Author Manuscript

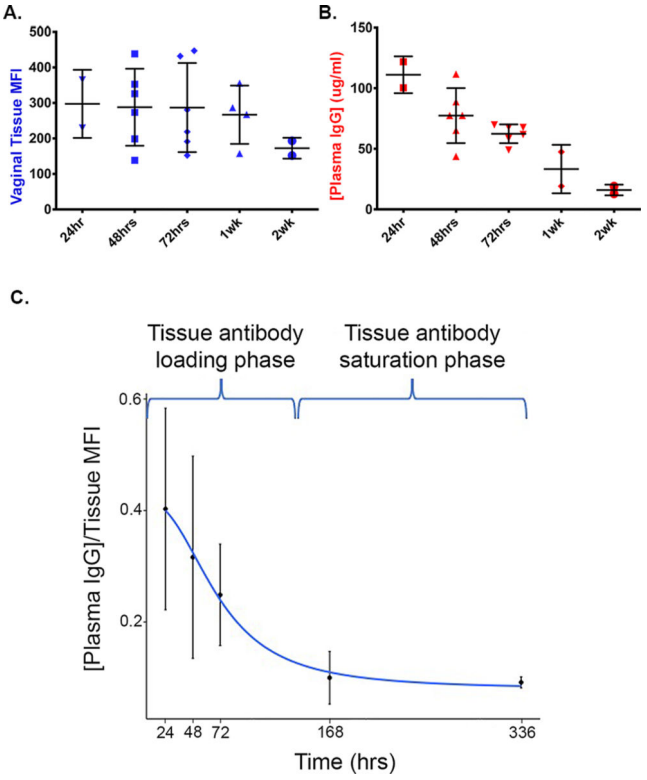

Figure 2: IV-injected fluorescently labeled antibodies persist in vaginal tissues as plasma concentration is decreased.

(A) Temporal analyses of mean fluorescent intensities (MFI) of VRC01-WT-Cy3 and VRC01-WT-Cy5 within the lamina propria of rhesus macaque vaginal tissues. Each displayed dot represents the average MFI from 11 panel images per animal from each time point. (B) Antibody concentrations for VRC01-WT-Cy3 and VRC01-WT-Cy5 over time for plasma. Each sample was run in triplicate and each displayed dot represents the average per animal from each time point. (C) The ratio of mean antibody plasma concentrations versus vaginal tissue MFI. A four-parameter log-logistic function was used as the best-fitted function to model the ratio decay (blue line).